Appl. Phys. A 49, 365–377 (1989)

Applied Physics A Solids and Surfaces

Spectroscopy of Image-Potential States by Two-Photon Photoemission

W. Steinmann

Sektion Physik, Universität München, Schellingstrasse 4, D-8000 München 40, Fed. Rep. Germany

Received 12 May 1989/Accepted 2 June 1989

Abstract. Unoccupied electronic states in solids and at solid surfaces are usually studied by inverse photoemission. An alternative method is two-photon photoemission. It is superior in resolution but limited to states of sufficiently long lifetime below the vacuum level. So far this method has mainly been applied to image-potential states on metal surfaces. On Ag(111) and Cu(111) a narrow surface state below the Fermi level serves as the initial state, which results in a pronounced resonance in the two-photon photoemission. Ni(111) shows similar results. In the resonance the image-potential state is so highly populated that electron–electron interaction leads to an Auger-type process. Nevertheless, the system is not so greatly disturbed as to show deviations from the one-photon photoemission results concerning the occupied states. Ag(100) and Cu(100) have a smooth continuum of initial states. Consequently, no resonance occurs. The binding energy does not depend on the material but changes with surface orientation: it is about 0.80 eV at the (111) surfaces and about 0.55 eV at the (100) surfaces. The effective mass is free electron like except on Ag(111), where it is 30% heavier. The lifetime on Ag(100) is about 20 fs. The agreement with theory is excellent in some cases and only fair in others.

PACS: 73.20Cw, 79.60Cn, 79.20Ds

Photoelectron spectroscopy has been developed over the last quarter century as the most powerful method for investigating electronic states in solids, both in the bulk and at the surface. It is specially suited for studying occupied states (Fig. 1a). In certain cases, information about the final state can also be obtained. Obviously the energy range between the Fermi energy and the vacuum energy is inaccessible by this method.

Unoccupied electronic states can be studied by inverse photoemission (Fig. 1b). This method, which was invented some years ago, has since been applied extensively to investigate bulk and surface states below and above the vacuum level [1–3]. The resolution is not as good as in photoelectron spectroscopy, as it is limited by the thermal energy distribution of the incoming electron beam.

An alternative to inverse photoemission is two-photon photoemission (Fig. 1c). In contrast to (one-photon) photoemission, it involves, in addition to an initial and a final state, an intermediate state. Therefore it yields information about the intermediate state involved in the process. The two photons need not have the same energy. If two photons of different energy are employed, additional information can be obtained. Most of the experiments on two-photon photoemission and all but one of the measurements reported in this paper have used a single, monochromatic photon beam, thus two photons of the same energy.

The advantage of two-photon photoemission is better resolution, which is as good as in one-photon photoemission. It is, however, subject to some limitations compared to inverse photoemission. The lifetime of the intermediate state has to be sufficiently long. There are examples of unoccupied states [e.g. at Cu(110) surfaces] which have been seen in inverse photoemission [4] but could not be detected in two-photon photoemission [5], presumably because the lifetime was too short. Another limitation concerns the photon energy, which must not exceed the work

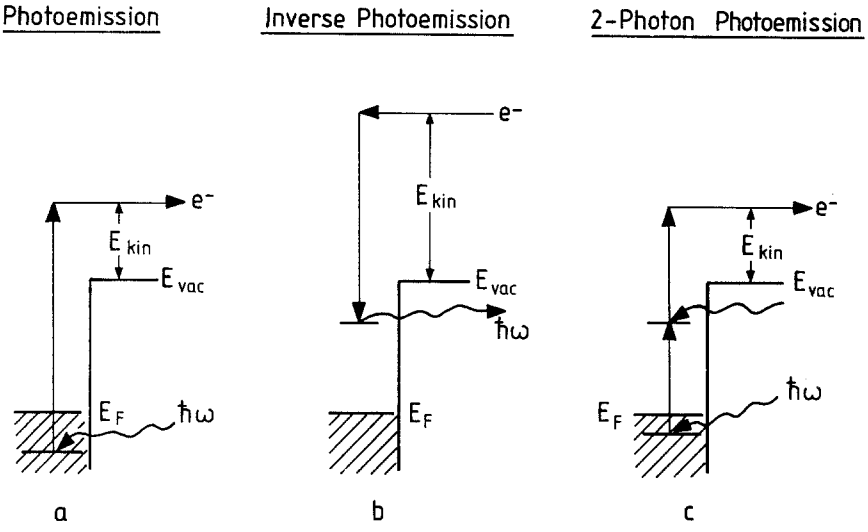

Fig. 1. a Photoemission: a photon of known energy $\hbar\omega$ excites an electron from an initial state below the Fermi energy E_F to a final state above the vacuum energy E_{vac}. The kinetic energy E_{kin} of the emitted electron is measured and with the work function $\phi = E_{vac} - E_F$ and $\hbar\omega$ the energy of the initial state with respect to E_F can be determined. **b** Inverse photoemission: electrons with known kinetic energy impinge on a solid where they make a radiative transition to an unoccupied state. The energy $\hbar\omega$ of the photons emitted in this process is measured and the energy of the final state can be determined. **c** Two-photon photoemission: a photon of known energy $\hbar\omega$ excites an electron from an occupied initial state to an unoccupied intermediate state. A second photon of the same or of different energy excites the electron from the intermediate state to the final state above E_{vac}. The kinetic energy of the emitted electron is measured and, with the photon energies, the energies of the intermediate and initial states can be determined

function. One-photon photoemission leads to excessive space charge, which distorts the energy distribution of the two-photon photoelectrons. Consequently, the intermediate states are limited to the range between E_F and E_{vac}; this condition, however, is necessary but not sufficient, which becomes obvious if, for some reason, the initial state lies well below E_F.

Strictly speaking, the situation in inverse photoemission and in two-photon photoemission is different: inverse photoemission starts with an n-electron system in the ground state and leads to an $(n+1)$-electron system, whereas the intermediate state of a two-photon photoemission-process is an $(n-1)$-electron system and an electron–hole pair. Consequently, the results of the two experiments need not necessarily be the same. The difference seems to be too small to be detected with the present limits of error of the two methods. Two-photon photoemission has been used to study bulk and surface states in a number of solids. This paper reports the investigation of image-potential states at metal surfaces.

1. Experimental

The light intensity in a two-photon photoemission experiment has to be high enough to have a finite probability of exciting an electron from the intermediate state. This can only be achieved with a pulsed laser beam. The experimental arrangement used for most of the measurements reported in this paper is shown in Fig. 2. A tunable two-stage dye laser is pumped by a XeCl excimer laser with a repetition rate of up to 50 Hz. After frequency doubling a monochromatic beam with photon energy up to 5.5 eV is available. The intensity is monitored by a photodiode. The beam is focused onto the sample surface, the angle of incidence being 45°. The light is polarized in the plane of incidence. The light spot on the surface has typically a diameter of around 0.1 mm. The light intensity is limited to less than 5×10^4 W/cm^2 in order to avoid space charge, which leads to a distortion of the energy distribution. The reflected beam leaves the sample chamber through a second window. A lens projects an image of the sample surface onto a screen. This allows one to observe the sample area under investigation and to choose a part free of pits and scratches, which lead to stray light and to spurious signals. The sample is prepared and kept in an UHV chamber equipped with an argon ion gun for cleaning the surface. The chemical composition can be checked by Auger electron spectroscopy and the structure by LEED.

Electrons emitted normal to the surface are focused onto the entrance aperture of a hemispherical electron analyzer with good energy (50 meV) and angular (2°) resolution. In addition to two-photon photoemission, one-photon photoemission of the sample can be

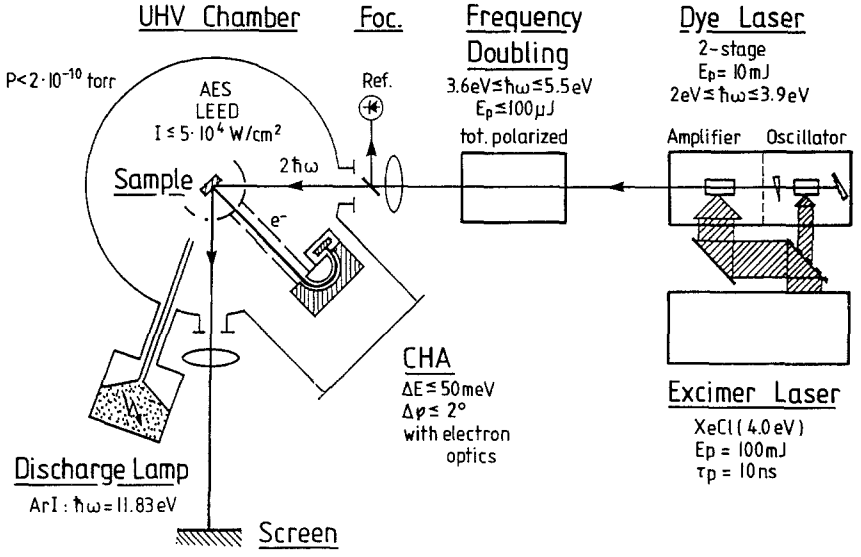

Fig. 2. Experimental arrangement for two-photon photoemission spectroscopy [6]

measured in situ, using the same analyzer. A gas discharge lamp is used in these measurements. With these photoelectron spectra the initial state density distribution, the Fermi energy and the work function are determined. Instead of He, commonly used in such measurements, the lamp was operated with Ar for most of the experiments reported in this paper, because of the lower photon energy, as the cross section of the surface states at the (111) surface of Cu and Ag increases with decreasing photon energy.

2. Image-Potential States

In a two-photon photoemission experiment, the lifetime of the electron in the intermediate state should be as long as possible. This leads to a high population and thus to a strong signal, which facilitates the detection of the structure related to the intermediate state in the photoelectron energy distribution. Of all electronic states in solids or at solid surfaces, image-potential states are expected to have the longest lifetime. They are confined to the space between the crystal surface and the image-potential, which describes the electrostatic force acting on an electron that leaves the surface (Fig. 3). An electron in an image-potential state is outside the solid, some tenths of a nanometer in front of the surface. Therefore electron–electron and electron–phonon interactions are much weaker than in the bulk and even in other surface intermediate states.

Image-potential states were predicted a long time ago [7–9] but were detected by inverse photoemission spectroscopy only fairly recently [10, 11]. A stationary image-potential state must not be degenerate with a bulk state of the same wave vector k parallel to the surface (which is conserved when an electron crosses the surface). In this case an electron in an image-potential state cannot enter the solid and is caught in the potential cage formed by the image-potential and the surface. As the image potential varies as $1/z$, the system is, in the lowest approximation, hydrogenic, and the image-potential states form a Rydberg series with 1/16 the eigenvalue of the H atom. Thus the binding energy (relative to the vacuum energy) of the $n=1$ state is 1/16 Ry = 850 meV in this approximation.

2.1. (111) *Surfaces*

Image-potential states have been detected by inverse photoemission at a number of (100) (110), and (111)

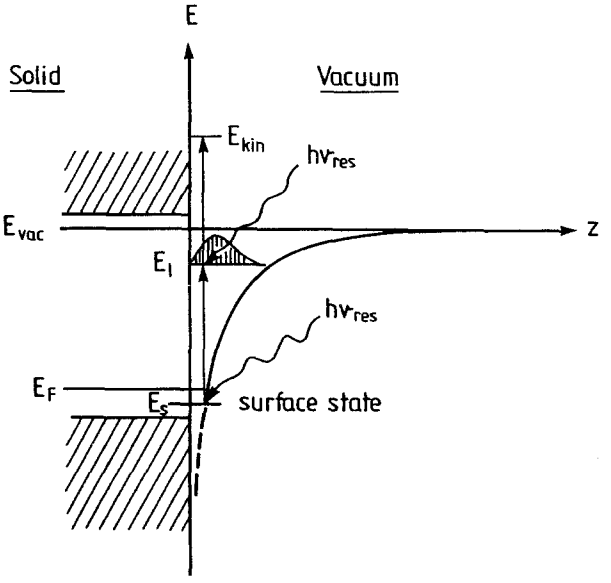

Fig. 3. Schematic of the Cu(111) surface showing the band structure, the image-potential and the resonant two-photon photoemission from the surface state E_S via the $n=1$ image-potential state E_1

surfaces of metals [12], although the condition that the image-potential state is not degenerate with bulk states is fulfilled only for the (100) and (111) surfaces of certain metals, e.g., Cu and Ag. At the (111) surfaces, the gap of the bulk states with $k_{||}=0$ extends below E_F. This results in a narrow surface state between E_F and the bottom of the gap. This situation is advantageous for a two-photon photoemission experiment for two reasons: (1) The surface state has an appreciable overlap with the image-potential state leading to a high transition probability if used as an initial state. (2) As the surface state is narrow and a much smaller population of the image-potential state is expected from initial states of higher and lower energy, due to lack of density and lack of overlap, a pronounced resonance should occur when the photon energy is tuned to the difference between the image-potential state and the surface state (Fig. 3). This resonance has been observed in the two-photon photoemission spectra from the (111) surfaces of Cu, Ag, and Ni [6].

Cu(111). Figure 4 shows the one-photon photoemission spectrum (EDC) of Cu(111). The double structure between 6 and 7 eV kinetic energy is related to the surface state. The splitting is due to the two lines emitted by the Ar discharge, which are caused by spin–orbit splitting. The structure between 3 and 5 eV is related to the *d*-bands. The surface state has a positive dispersion. Thus at some (rather small) $k_{||}>0$ the dispersion curve crosses E_F and for larger $k_{||}$ the surface state is unoccupied and hence no longer visible in the one-photon EDC. A tilting of the sample by 13° is sufficient to achieve this and the EDC at this angle of

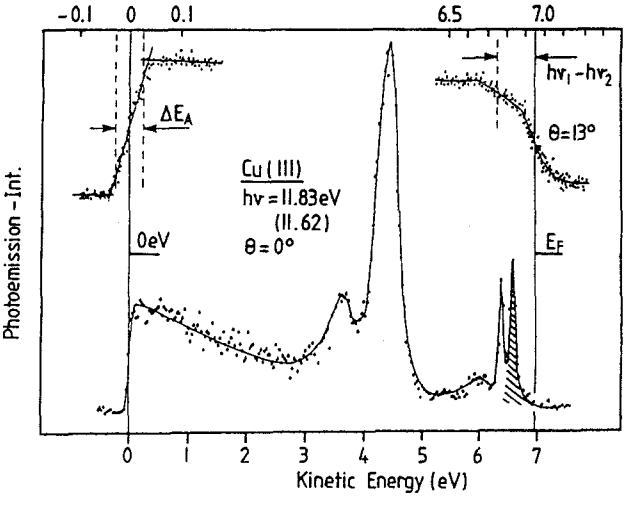

Fig. 4. One-photon photoelectron energy distribution from Cu(111) [6]. The hatched peak is due to electrons excited from the surface state by 11.83 eV photons. The insets in the upper half show, on an expanded energy scale, the low energy cutoff, indicating the analyzer resolution $\Delta E_A=50$ meV and the Fermi edge measured at an emission angle of 13° to the normal

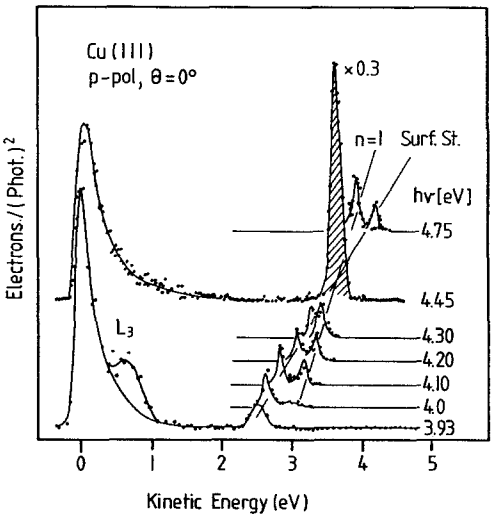

Fig. 5. Two-photon photoemission spectra (EDC) from Cu(111) for various photon energies [6]. The hatched peak is caused by the resonance excitation from the surface state via the image-potential state. The structure designated L_3 is due to excitation from the *d*-band. The lines designated "$n=1$" and "Surf. St." are explained in Figs. 7 and 8 and the related text

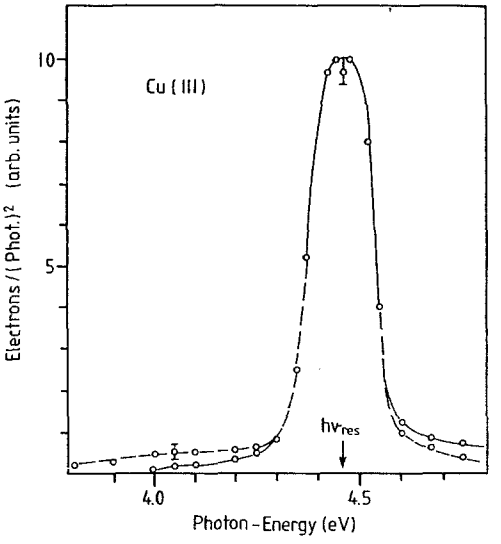

Fig. 6. Resonance curve showing the peak height of the high energy structure of Fig. 5 as a function of photon energy [6]. Off resonance, the dashed curve corresponds to the peak on the "Surf. St." line

emission allows a precise determination of E_F. This result in combination with the low energy cutoff is used to determine the work function.

The two-photon photoemission spectra of Cu(111) (Fig. 5) show the expected resonance at a photon energy of 4.45 eV, whereas at lower and higher photon energies the structure related to the image-potential state is much smaller and splits into two peaks. The resonance curve (Fig. 6) shows that with the resonance

photon energy $h\nu_{res}$ the peak height of the image-potential peak is enhanced by two orders of magnitude.

The binding energy of the $n=1$ image-potential state $E_{B1}=E_{vac}-E_1$ (Fig. 3) is readily obtained from the resonance photon energy and the kinetic energy:

$$E_{B1}=h\nu_{res}-E_{kin}. \quad (1)$$

The position of the initial state E_S can also be determined by the two-photon photoemission experiment:

$$E_S=E_1-h\nu_{res}. \quad (2)$$

Hence the binding energy of the surface state with respect to the Fermi energy is

$$E_{BS}=E_F-E_S=2h\nu_{res}-E_{kin}-\phi, \quad (3)$$

where $\phi=E_{vac}-E_F$ is the work function determined from the one-photon photoelectron spectrum (Fig. 4). On the other hand, E_{BS} can also be found from one-photon photoemission (Fig. 4). The results obtained independently from one- and two-photon photoemission are identical within the limits of error. This is proof that the disturbance of the electronic system of the sample caused by the rather intense photon pulse used in two-photon photoemission is not noticeably greater than in one-photon photoemission excited by a much weaker intensity. Thus, for the discussion of the data obtained by two-photon photoemission we can use the band structure of the one-electron theory and the results of one-photon photoelectron spectroscopy.

A peak in a two-photon photoemission spectrum may be related to an initial state or to an intermediate state. The two cases can be distinguished by studying how the peak shifts with photon energy. If the peak is caused by a fixed initial state, the intermediate state must shift with photon energy and the final state will shift twice as much as the photon energy:

$\Delta E_{kin}=2\Delta h\nu$ for fixed initial state.

If a peak is caused by a fixed intermediate state, the initial state shifts downward while the final state shifts upward with increasing photon energy:

$\Delta E_{kin}=\Delta h\nu$ for fixed intermediate state.

In a plot of the peak position versus photon energy (Fig. 7) the data points lie on straight lines. For a fixed initial state the line has a slope of 2, for fixed intermediate states a slope of 1.

For Cu(111) this plot (Fig. 7) shows two lines with slope 2. The lower one demonstrates the shift of the peak denoted L_3 in Fig. 5 and is related to a critical point in the d-bands. The upper line with slope 2 corresponds to transitions from the surface state below

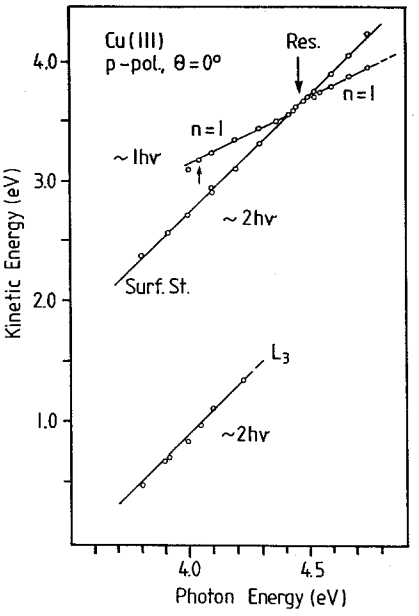

Fig. 7. Peak position versus photon energy for the spectra shown in Fig. 5 [6]

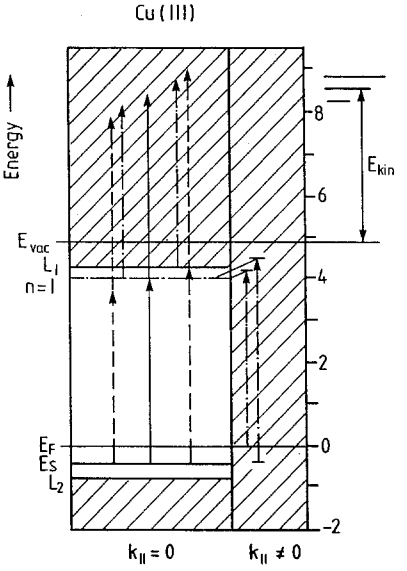

Fig. 8. Transitions causing the peaks shown in Fig. 5 and plotted in Fig. 7. The image-potential state is designated "$n=1$". Solid arrows: resonance transition; dashed arrows: off-resonance transitions from surface state as fixed initial state; dash-dotted arrows: off-resonance transitions via the image-potential state as fixed intermediate state

E_F. In addition, there is a line with slope 1 denoted $n=1$. It is caused by the $n=1$ image-potential state as a fixed intermediate state. It crosses the line related to the surface state as a fixed initial state at the resonance photon energy. This explains the splitting of the peak at off-resonance photon energies shown in Fig. 5.

The transitions giving rise to the data plotted in Fig. 7 are indicated in Fig. 8. Two remarks should be

made: (1) Transitions from the surface state as the fixed initial state have, for off-resonance photon energy, no allowed intermediate state. In an atom, this would reduce the transition probability by many orders of magnitude. At a crystal surface, however, the electronic states in the gap are not strictly forbidden. Their lifetime is merely reduced compared to allowed states, noticeably but not drastically. The off-resonance peak heights shown in Figs. 5 and 6 can be quantitatively accounted for in this way. (2) Transitions involving the $n=1$ image-potential state as a fixed intermediate state are more complicated. For off-resonance photon energies, in addition to $k_{||}$-conserving transitions starting from the surface state and involving relaxations (process B in Fig. 11), transitions are possible, and may be more probable, that do not conserve $k_{||}$. They start from allowed bulk initial states, lead to allowed intermediate states from which the electron is scattered by phonons or electrons into the image-potential state. This transition is, however, not possible for $h\nu < E_1 - E_F$. This is confirmed by the experimental data: in Fig. 6 the solid curve, which shows the peak height for fixed intermediate state, goes to zero for $h\nu = 4$ eV, in agreement with $E_{BS} = 0.41$ eV.

Ag(111). The situation concerning the electronic levels at the Ag(111) surface [13] is very similar to Cu(111) (Fig. 9). There is however a noteworthy difference: the binding energy of the surface state is smaller by one order of magnitude. [Ag(111): $E_{BS} = 40$ meV, Cu(111): $E_{BS} = 410$ meV]. This causes remarkable differences in the experimental findings.

The resonance photon energy, corresponding to the transition from the surface state to the image-potential state, is 3.84 eV for Ag(111) (Fig. 10). As the photon energy is increased, the peak A_1 caused by the resonant transition rapidly decreases in height (Fig. 12) and splits into two and for $h\nu > 4.39$ eV into three peaks. The position of the peak B_1 shifts with

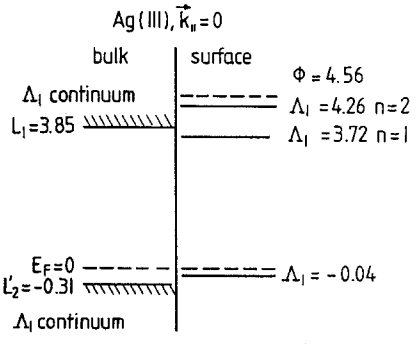

Fig. 9. Energy diagram for electronic states with $k_{||}=0$ at the Ag(111) surface [13]. The energies are given in eV relative to E_F. The A_1 state at $E=-0.04$ eV is the surface state. $n=1$ and $n=2$ designate the respective image-potential states

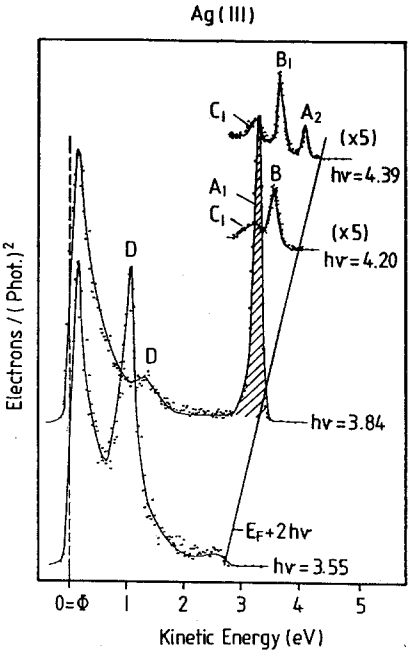

Fig. 10. Two-photon photoemission spectra (EDC) from Ag(111) for various photon energies [13]. The hatched peak A_1 is caused by the resonance transition from the surface state via the ($n=1$) image-potential state (A in Fig. 11). Peak D is of unknown origin and has been tentatively assigned to a surface state on Ag(110) facets that has been observed with inverse photoemission on Ag(110)

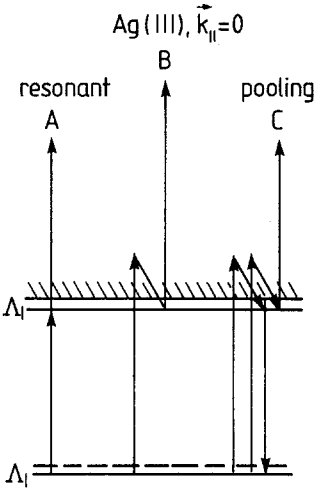

Fig. 11. Two-photon processes used to account for the spectra shown in Fig. 10. *A:* Resonant transition. *B:* Off-resonant transition from surface state via image-potential state with relaxation. *C:* Off-resonant energy pooling process. (From [13])

increasing photon energy as $\Delta E_{B1} = \Delta h\nu$. Thus the peak B_1 is caused by transitions via the $n=1$ image-potential state as the fixed intermediate state. One possibility for this transition is the three-step process indicated in Fig. 11: an electron is excited from the surface state to the continuum of the allowed bulk states above the gap and subsequently scattered into

the image-potential state, from where it is excited to the final state above E_{vac} by a second photon.

The second peak, designated C_1, does not shift with photon energy. This is to be expected for transitions to fixed final states, but there is no reason why such transitions should occur in this case. An alternative explanation is indicated in Fig. 11: two electrons in the image-potential state interact as in an Auger process, one electron returning to the ground state gives its energy to the second electron, which is emitted, giving rise to the peak C_1. This process was named energy pooling [13], as the term Auger process refers to transitions involving occupied electronic states.

Energy pooling requires a rather high electron density in the image-potential state. It should be borne in mind that energy pooling can only be observed above resonance, where the image-potential state is populated via the relaxation process B. A much higher density will be achieved in the resonant transition A, where the pooling peak C_1 and the resonance peak A_1 coincide. Thus in the resonance a high-density two-dimensional electron gas is created in front of the surface. The conductivity of this electron gas should be considerably higher than in the substrate crystal, as the electron–phonon interaction is expected to be much weaker. It seems tempting to do experiments with this electron gas but nothing has been reported so far.

The energy pooling process has to be k-conserving. The electron is emitted normal to the surface. Hence the ground state to which the second electron returns has to be at $k_{||}=0$. The only possible ground state is the surface state. Its binding energy [40 meV for Ag(111)] is comparable with kT at room temperature. Thus the surface state will be partially empty. Consequently the height of peak C_1 should depend rather sensitively on the sample temperature. But the temperature dependence of two-photon photoemission has not yet been studied. In Cu(111) the binding energy of the surface state is 410 eV; this explains why energy pooling was not observed with Cu(111).

The peak A_2, which occurs at $h\nu=4.39$ eV (Fig. 10), shows the same resonance behavior as A_1 (Fig. 12). It is caused by transitions via the $n=2$ image-potential state as intermediate. For $n=2$, the resonance photon energy, and hence the binding energy, corresponds, within the limits of error, to the prediction of the simple hydrogenic model, while for $n=1$ the binding energy (770 meV) is about 10% smaller than the hydrogenic value. This is to be expected, since for $n=1$ the electron stays closer to the surface, and therefore deviations from the $1/z$ dependence of the image-potential, which necessarily occur in the vicinity of the surface, have a larger effect.

As the photon energy is further increased, the height of the peak A_2 first decreases but then grows

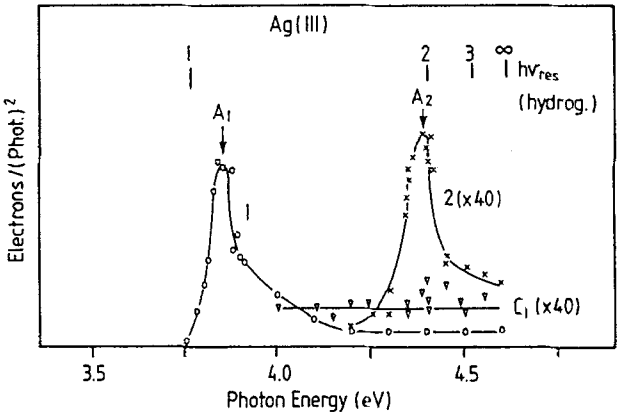

Fig. 12. Resonance curve (peak height as a function of photon energy) for the peaks $A_1(B_1)$ and $A_2(B_2)$ shown in Fig. 10. The height of C_1 is independent of photon energy, as expected. The resonance photon energies for the simple hydrogenic model are indicated at the top [13]

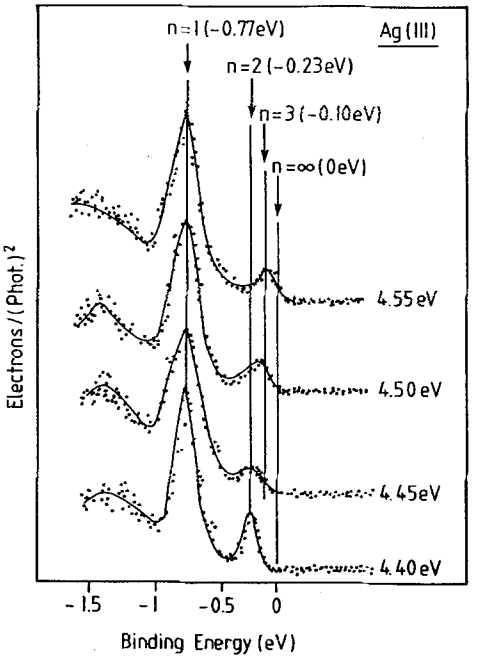

Fig. 13. Two-photon photoemission spectra from Ag(111) for four photon energies between the resonance energy for $n=2$ (4.40 eV) and for $n=3$ (4.55 eV) [6]

again (Fig. 13), but in a different position. This is caused by the resonant transition to the $n=3$ image-potential state. A_2 and A_3 cannot be resolved, but the binding energy of the $n=3$ image-potential state can be determined from the peak position at $h\nu=4.55$ eV.

The second and third members of the Rydberg series could be observed for Ag(111) because the binding energy of the surface state (40 meV) is smaller than the binding energy for $n=3$. Therefore the resonance photon energy for $n=3$ is smaller than the work function and no one-photon photoemission

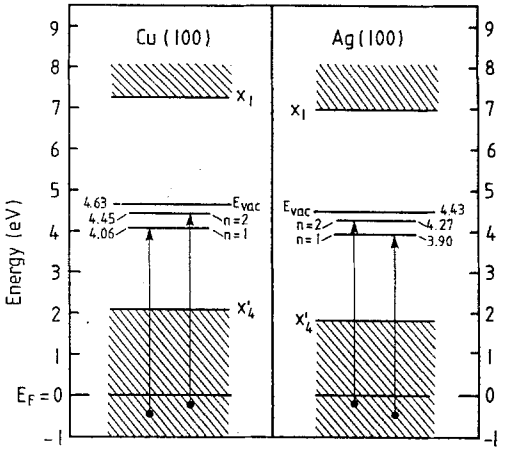

Fig. 14. Energy diagram for electronic states at the Cu(100) and Ag(100) for $k_{||}=0$. Hatched areas indicate projected bulk band continua

disturbs the two-photon photoemission experiment. For Cu(111) the binding energy of the surface state (410 meV) exceeds that of the $n=2$ image-potential state by 200 meV. Consequently, at the $n=2$ resonance, one-photon photoemission leads to excessive space charge, which distorts the photoelectron spectrum.

The $n=2$ and $n=3$ image-potential states are degenerate with allowed bulk states (Fig. 9). Thus the condition for a stationary image-potential state is not fulfilled. Nevertheless, the corresponding peaks are clearly visible and as narrow as the peak A_1 caused by the $n=1$ state. The $n=2$ resonance is equally pronounced (Fig. 12). Obviously, degeneracy with bulk states does not affect these image-potential states very much.

Ni(111). The band structure of Ni is qualitatively different from Cu and Ag: the Fermi level lies within the *d*-band. Consequently, there is no gap around E_F in the (111) direction. The narrow surface state found at Cu(111) and Ag(111) is a much broader surface resonance degenerate with allowed *d*-states at Ni(111). Nevertheless, the results of two-photon photoemission experiments at Ni(111) are very similar to those of Cu(111) [6]: a pronounced, though somewhat broader resonance, and a narrow peak in the two-photon photoelectron spectrum, higher than the low energy maximum. The binding energy of the image-potential state (810 meV) is close to the hydrogenic value, and lies between the result for Cu(111) (830 meV) and Ag(111) (770 meV). Thus on the basis of the two-photon photoemission data obtained from the (111) surfaces we summarize that the binding energy of the image-potential states hardly depends on the material and is not sensitive to the details of the band structure.

2.2. (100) *Surfaces*

The band structure in the (100) direction of Cu and Ag is quite different from the situation in the (111) direction. There is a gap of about the same width (5 eV) but it is shifted upward by approximately 2 eV. Consequently a continuum of allowed bulk states extends to both sides of the Fermi level, and the vacuum level is located close to the center of the gap, while it lies at the top of or even above the gap at the (111) faces (Fig. 14). Thus there is no surface state or surface resonance below E_F at the (100) surfaces of Cu and Ag. Hence no resonance can occur in the two-photon photoemission and the peak related to the image-potential state is reduced for two reasons: (1) The density of initial states in the continuum is much lower than in the narrow surface state. (2) The transition probability from a bulk state to an image-potential state is smaller since the overlap of the wavefunctions is reduced. The experimental results shown in Fig. 15 verify these expectations: the peak height of the image-potential state is reduced by more than one order of magnitude compared to the resonance at the (111) surface. The (100) spectra are similar to the off-resonance situation at (111) surfaces. With photon energies close to the work function ($\phi - h\nu = 80$ meV), two members of the Rydberg series can be observed (Fig. 16). The binding energies, which can be found from the spectra as shown for the (111) surfaces in (1) are measurably smaller for the (100)

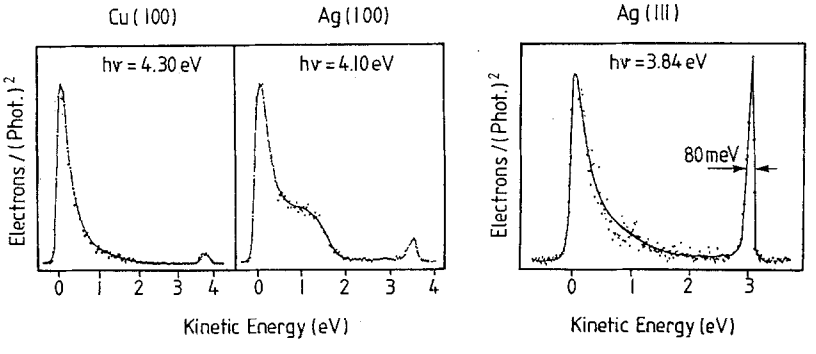

Fig. 15. Two-photon photoemission spectrum (EDC) from Cu(100) and Ag(100) at $k_{||}=0$ [14]. For comparison, the resonance EDC for Ag(111) is also shown. With these photon energies only the $n=1$ image-potential state can be populated

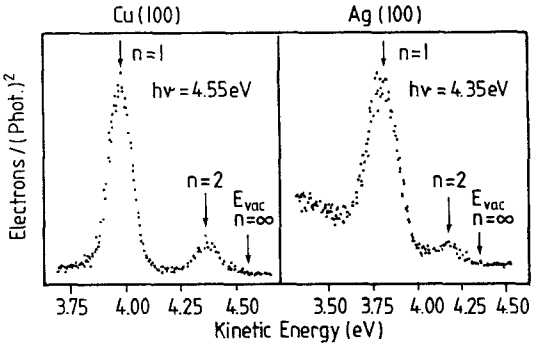

Fig. 16. Two-photon photoemission spectrum from Cu(100) and Ag(100) at $k_{\|}=0$ with $h\nu > E(n=2)-E_F$ showing the first two members of the Rydberg series [14]

surfaces. The binding energy of the $n=1$ state is about 2/3 of the hydrogenic number [530 meV for Ag(100) and 570 meV for Cu(100)], while for the $n=2$ state it is 4/5 [160 meV for Ag(100) and 180 meV for Cu(100)].

2.3. Dispersion

When the sample is slightly tilted, two-photon photoemission at oblique angles of emission can be observed. In this way the dispersion $E_B(k_{\|})$ of the image-potential states can be determined [15] (Fig. 17). This is a straightforward experiment with Cu(100) and Ag(100), since the initial states in this case form a smooth continuum. For Cu(111) and Ag(111) the surface state that serves as the initial state also has a dispersion. This will influence the result and lead to erroneous conclusions if the experiment is made with the resonance photon energy for $k_{\|}=0$. This has been done for Cu(111), where an angular dependence of the peak position corresponding to an effective mass $m^*/m=1$ has been measured [16]. The dispersion of the surface state below E_F is known from one-photon photoemission to be $m^*/m=0.5$ [17]. If the photon energy is in resonance for $k_{\|}=0$, it will go off resonance for $k_{\|}>0$. Assume that the dispersion of the image-potential state is $m^*/m=1.5$ and its width is the same as that of the surface state, then with increasing $k_{\|}$ the transition will take place from the high energy slope of the surface state to the low energy slope of the image-potential state and the dispersion observed will be midway between the dispersion of the two states involved, i.e. $m^*/m=1$.

In the spectra for Ag(111) shown in Fig. 17 this problem has been avoided by measuring off-resonance [16]. The spectra show the angular dependence of the peak B_1 in Fig. 10, which corresponds to a three-step process in which the image-potential state is populated indirectly via a relaxation or scattering following the

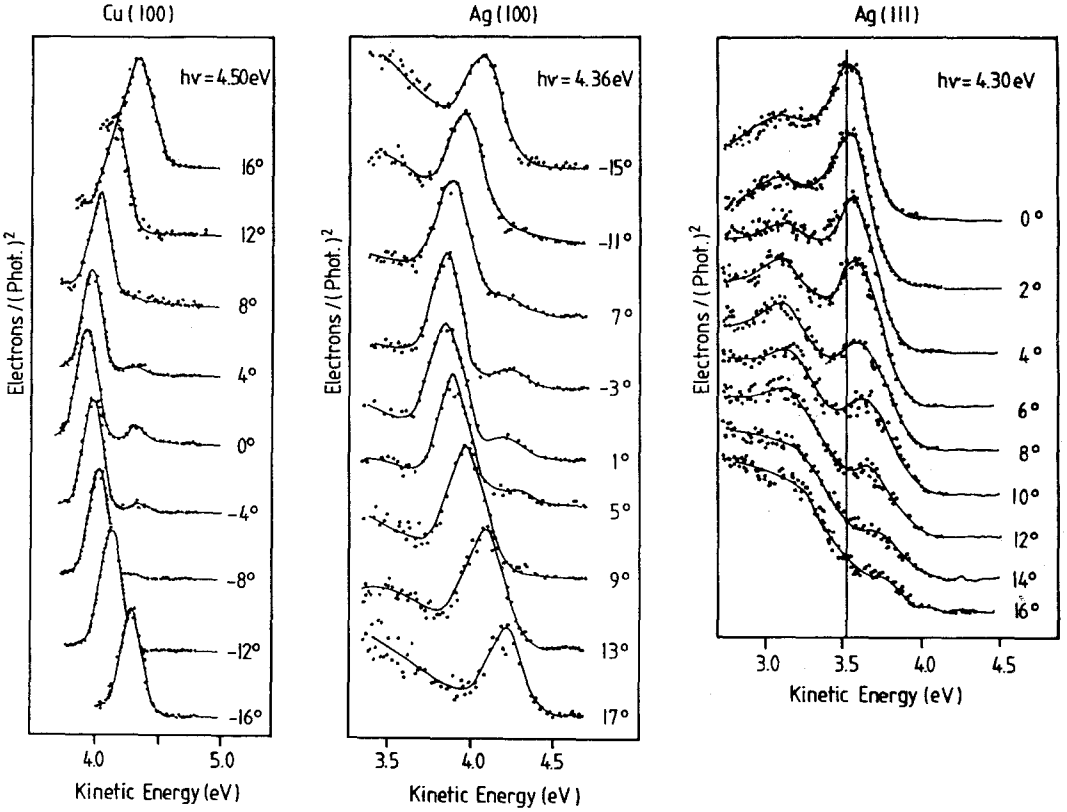

Fig. 17. Two-photon photoemission spectra from Cu(100), Ag(100), and Ag(111) for various emission angles, showing the dispersion of the $n=1$ image-potential state [15]

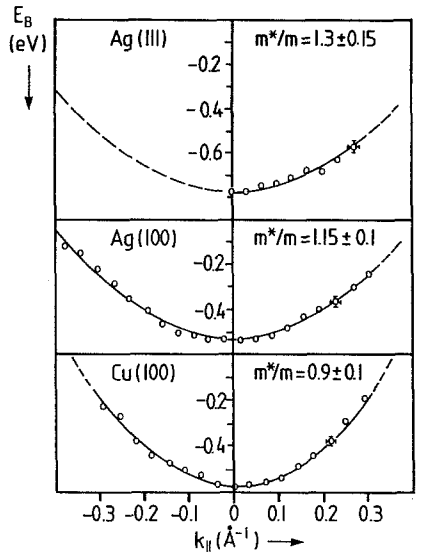

Fig. 18. Dispersion E_B vs $k_{||}$ for the $n=1$ image-potential state on Ag(111), Ag(100), and Cu(100). The data points are fitted by the parabolas corresponding to the indicated m^*/m (From [15])

first excitation of an occupied surface or bulk state. As the two-step process that populates the image-potential state is not k-conserving, the angular dependence shown in Fig. 17 is not influenced by the dispersion of the initial state. The peak positions $E_B(k_{||})$ for Cu(100), Ag(100), and Ag(111) are shown in Fig. 18. For Cu(100) and Ag(100) the effective masses are equal or close to 1 within the limits of error, while for Ag(111) the effective mass is markedly greater. These results of two-photon photoemission spectroscopy are (within the limits of error) in agreement with inverse photoemission data.

The dispersion of the image-potential state at (111) surfaces can be measured in resonance (i.e. with a stronger signal) if, for each angle of emission, i.e. for each $k_{||}$, the photon energy is tuned to resonance and the resonance photon energy determined. With the dispersion of the initial state known from one-photon photoemission, the dispersion of the intermediate state would be readily found. This method has recently been used to determine the dispersion of the $n=1$ image-potential state of a Ni(111) surface [18]. In this case the initial state, a surface resonance, is considerably broader than the surface state at Cu(111) and Ag(111) and hence the tuning is less critical. A careful investigation of the angular dependence led to the conclusion that for Ni(111) the effective mass of the $n=1$ image-potential state is $m^*/m=1.1\pm0.1$. This result is not in agreement with inverse photoemission data, which showed $m^*/m=1.6$ for Ni(111) [19].

2.4. *Lifetime*

Electrons in image-potential states are only weakly interacting with the crystal. Therefore they should have a much longer lifetime than electrons in excited states in the bulk. The high density required for the energy pooling process found with Ag(111) has been achieved with a laser pulse width of 10^{-8} s. This suggests a lifetime orders of magnitude longer than in the bulk. Echenique et al. [20] have calculated the lifetime of image-potential states. For Ag(100) they find that the natural linewidth for $k_{||}=0$ is $\Delta E<10$ meV. This corresponds to a lifetime $\tau>7\times10^{-14}$ s. The only decay channel considered in this calculation is excitation of an electron–hole pair in the bulk.

The lifetime of the $n=1$ image-potential state on Ag(100) has recently been determined by Schoenlein et al. [21] in a time-resolved two-photon photoemission experiment using femtosecond laser pulses. The image-potential state was populated by a 4 eV photon and subsequently ionized by a 2 eV photon, which could be delayed on a femtosecond time scale. The decrease of peak height with increasing delay time was observed and the lifetime was found to be $15\text{ fs}<\tau<35$ fs.

The linewidth of the image-potential state can be found from the peak width in the two-photon photoemission spectrum if the resolution of the analyzer is known. This is obviously not possible if the initial state has a width comparable to or even narrower than the image-potential state, as is the case in the resonance excitation on Ag(111) and Cu(111). The peak in the one-photon photoelectron spectrum corresponding to the surface state below E_F has a width of 50 meV, which is mainly due to the resolution of the analyzer [13]. Thus two-photon photoemission will produce an equally narrow peak even if the intermediate state is much wider. This argument does not hold for off-resonance excitation via the image-potential state (see process B in Fig. 11) but in these experiments as well as with Cu(100) and Ag(100), analyzer speed was increased at the cost of resolution. Recently Matthias and coworkers [22] have measured the two-photon photoemission spectrum from Ag(100) with an analyzer resolution of 70 meV. They found a peak width of 78.6 ± 3.3 meV from which they deduced a linewidth of the image-potential state of 35 ± 9 meV. This corresponds to a lifetime of 20 ± 5 fs. Hence the experimental data indicate that the lifetime of the $n=1$ image-potential state on Ag(100) is less then half of the calculated value. This is presumably due to an additional decay channel, e.g., surface imperfections.

2.5. *Discussion of Binding Energies and Dispersions*

The experimental results concerning the binding energies obtained by two-photon photoemission are shown in Fig. 19 together with data of inverse photoemission. Due to the improved resolution (smaller limits

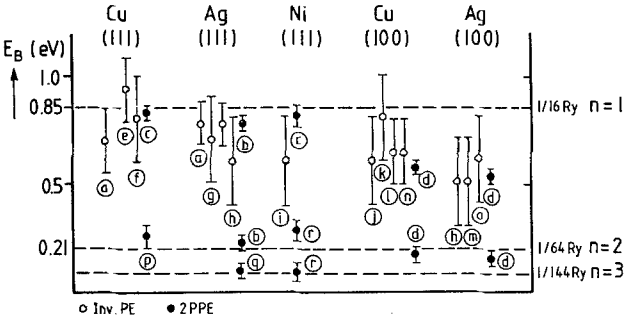

Fig. 19. Comparison of binding energies of image-potential states determined by inverse photoemission (open circles) and by two-photon photoemission (solid circles) References: a: [12]; b: [13]; c: [6]; d: [14]; e: [24]; f: [4]; g: [25]; h: [26]; i: [27]; j: [28]; k: [10]; l: [24]; m: [26]; n: [11]; o: [29]; p: [16]; q: [6]; r: [18]

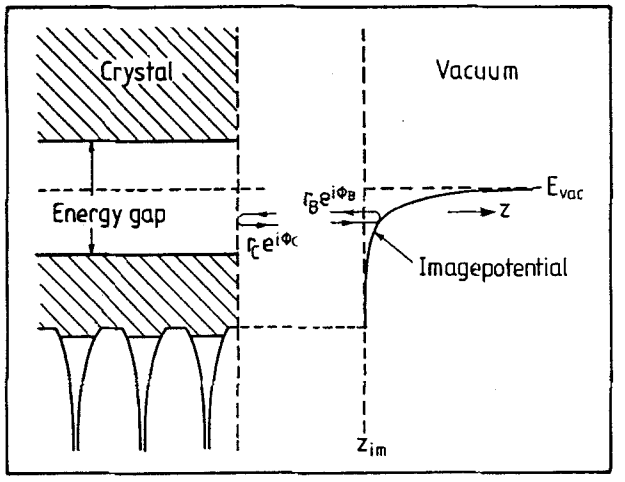

Fig. 20. Schematic potential in the vicinity of a crystal surface and reflection of the wavefunction of an electron caught in the potential cage. (See [23])

of error) the two-photon photoemission data clearly show that the binding energy hardly depends on the material as long as the surface structure remains constant but changes markedly with crystal structure: for the (111) surfaces, E_B is close to the hydrogenic value 0.85 eV, while for the (100) surfaces it is 30% lower [14].

This surprising effect is accounted for by a more refined theory [23] of the image-potential states. It is based on an analysis of the phase change which the electron wavefunction experiences when it is reflected at the crystal and at the image potential (Fig. 20). The condition for a stationary state is that the sum of the two phase changes is an integral multiple of 2π

$$\phi = \phi_B + \phi_C = 2\pi n .$$

The phase changes vary with energy: ϕ_C is zero at the bottom of the gap and reaches π at the top. Figure 21 demonstrates the situation for Cu(111) and

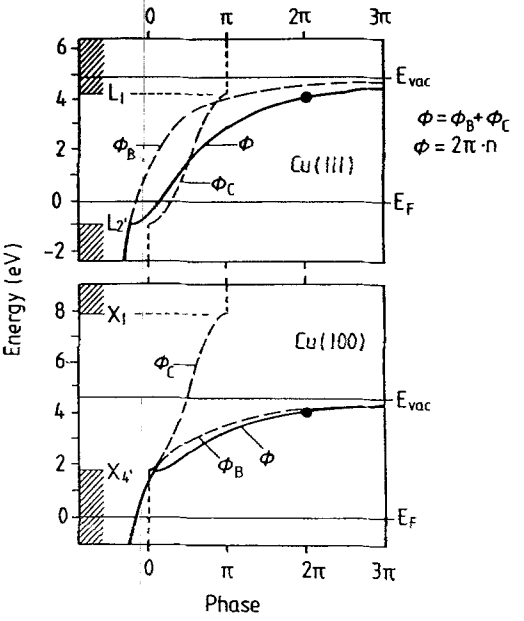

Fig. 21. Dependence of reflection phase changes on energy for Cu(111) and Cu(100). The symbols are explained in Fig. 20. (See [24])

Cu(100) and is also representative for Ag(111) and Ag(100). Obviously, the binding energy depends critically on the location of the vacuum level with respect to the gap. If the vacuum level lies close to the top of the gap, as is the case for (111) surfaces, $\phi_C = \phi_B = \pi$ is the condition for the $n=1$ state. If, however, the vacuum level lies in the middle of the gap, $\phi_C = \pi/2$ and hence $\phi_B = 3\pi/2$, which obviously results in a lower binding energy.

Quantitatively, the effect can be described by a quantum defect $a = (1/2)(1 - \phi_C/\pi)$, which is independent of n if ϕ_C is assumed to be constant over the range of the series. The binding energy is given by the modified Rydberg formula

$$E_B(n) = R/(n+a)^2 .$$

For $\phi_C = \pi$, $a = 0$ and the hydrogenic Rydberg series is expected. This explains the results found at the (111) surfaces. For the (100) surfaces, $\phi_C = \pi/2$ approximately, and $E_B(1) = 0.54$ eV, $E_B(2) = 0.17$ eV, in very good agreement with the experimental results. A more detailed quantitative comparison is shown in Table 1. For Ag and Cu the overall agreement is excellent.

Remarkable differences between theory and experiment occur, however, for Ni(111). The phase analysis predicts a binding energy 20% below the hydrogenic value, since the vacuum level is located markedly below the top of the gap (Fig. 22). But the results of the phase calculation shown in Fig. 21 are based on the assumption of p-states at the bottom and s-states at the top of the gap (Shockley inverted gap). This is not

Table 1. Binding energy [eV] and dispersion: comparison of phase analysis and experimental data

	Phase analysis			Experimental: two-photon photoemission						Inverse photoemission	
	$E_B(1)$	$E_B(2)$	m^*/m	$E_B(1)$	Ref.	$E_B(2)$	Ref.	m^*/m	Ref.	m^*/m	Ref.
Ag(111)	0.75	0.21	1.33	0.77±0.03	[13]	0.23±0.03	[13]	1.3±0.15	[15]	1.0	[25]
										1.4±0.3	[27]
Ag(100)	0.53	0.17	1.11	0.53±0.02	[14]	0.16±0.02	[14]	1.15±0.1	[15]	1.2±0.2	[27]
										1.5±0.1	[30]
Cu(111)	0.85	0.21	1.5	0.83±0.03	[6]	0.26±0.05	[16]	0.9±0.2	[16]	1.0	[4, 24]
Cu(100)	0.50	0.16	0.96	0.57±0.02	[14]	0.18±0.02	[14]	0.9±0.1	[15]	1.0	[4]
										1.2±0.2	[10, 28]
Ni(111)	0.69	0.19	1.0	0.81±0.03	[6]	0.27±0.03	[18]	1.1±0.1	[18]	1.6±0.2	[19]

applicable to Ni(111), as the states at the bottom of the gap are predominantly *d*-like. As yet, ϕ_C has not been calculated for this case. Even if such a calculation could resolve the disagreement about the $n=1$ state, it is questionable whether it could account for the binding energy of the $n=2$ state, which is higher than the hydrogenic value. It seems to be inconsistent with the rule of a Rydberg series and may therefore require a basically different theory.

The dispersion can also be calculated in the phase analysis model [15, 23]. For image-potential states located close to the top of the gap [Ag(111) and Cu(111)], $m^*/m>1$ is predicted. Otherwise the dispersion should be nearly free-electron-like. Table 1 shows quantitative agreement between the prediction of the phase analysis model and the results of two-photon photoemission for Ag(111), Ag(100), Cu(100), and Ni(111). The latter may be fortuitous in view of the disagreement in the binding energy and the explanation offered for it. The discrepancy for Cu(111) may be due to a systematic error in the experiment that is described in Sect. 2.3. The results of inverse photoemission concerning dispersion are also listed in Table 1, as their accuracy is comparable to the data of two-photon photoemission. For Cu(111) they do not agree with the result of the phase analysis. The discrepancy could be explained if the image-potential state lay above the gap [16], contrary to the assumption made in the phase analysis [23]. Some of the data for Ag(100) and Ni(111) indicate m^*/m discordant with the prediction of the phase analysis model and the results of two-photon photoemission. It has been speculated [30] that this discrepancy may be due to systematic differences between the two experimental methods that are mentioned at the beginning of this paper: the screening of the incoming electron in the case of inverse photoemission and of the electron–hole pair created in two-photon photoemission are acting in opposite directions and may thus be responsible for differing results. Further experiments and calculations are required to clarify this point.

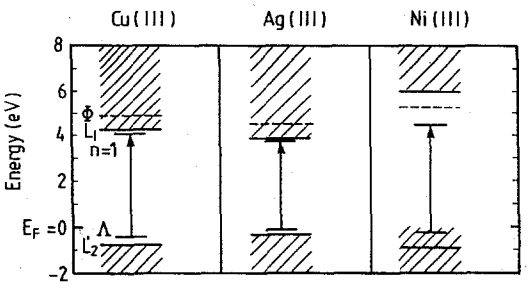

Fig. 22. Energy level diagram for $k_{||}=0$ for the (111) surfaces studied by two-photon photoemission. Hatched areas indicate bulk band continua

3. Further Applications of Two-Photon Photoemission Spectroscopy

The long lifetime of image-potential states facilitates the observation of two-photon photoemission. But this spectroscopy can also be applied to study other unoccupied electronic states of shorter lifetime. Adsorbate states have been measured in the system 0/Cu(111) [31]. An unoccupied state that had already been detected in inverse photoemission measurements was measured in two-photon photoemission with much higher accuracy. An occupied state known from one-photon photoelectron spectra could be determined more accurately and reliably in two-photon photoemission, presumably because it is more surface sensitive. Furthermore, bulk excited states that have an even shorter lifetime can be studied by two-photon photoemission. The first example [32] was a critical point at the *X* point in Cu, which was determined considerably more accurately than by inverse photoemission. It is expected that investigations of adsorbate states will become more and more important in future two-photon photoemission measurements.

Acknowledgements. Four years ago, F. J. Himpsel suggested applying two-photon photoemission spectroscopy to the study of image potential states on Ag(111) and Cu(111). This proposal led to the experiments reported in this paper. He has also contributed very much to the interpretation of the experimental results. Furthermore, I am grateful to him for many stimulating and clarifying discussions. F. Hage and K. Giesen built the experimental arrangement shown in Fig. 2 and performed most of the experiments. Interesting discussions with them as well as with E. Bertel, Th. Fauster, N. Fischer, W. Moritz, D. Rieger, S. Schuppler, N. V. Smith, K. Wandelt, and T. Wegehaupt are gratefully acknowledged. I am grateful to E. Matthias for making his results available prior to publication.

References

1. V. Dose: Surf. Sci. Rep. **5**, 337 (1985)
2. N.V. Smith, D.P. Woodruff: Prog. Surf. Sci. **21**, 295 (1986)
3. G. Borstel, G. Thörner: Surf. Sci. Rep. **8**, 1 (1988)
4. W. Jacob, V. Dose, U. Kolac, Th. Fauster: Z. Phys. B **63**, 459 (1986)
5. N. Fischer: Unpublished
6. K. Giesen, F. Hage, F.J. Himpsel, H.J. Riess, W. Steinmann: Phys. Rev. B **33**, 5241 (1986)
   K. Giesen: Doctoral Thesis, München (1986)
   F. Hage: Doctoral Thesis, München (1986)
7. M.W. Cole, M.H. Cohen: Phys. Rev. Lett. **23**, 1238 (1969)
8. N. Garcia, J. Solana: Surf. Sci. **36**, 262 (1973)
9. P.M. Echenique, J.B. Pendry: J. Phys. C **11**, 2065 (1978)
10. V. Dose, W. Altmann, A. Goldmann, U. Kolac, J. Rogozik: Phys. Rev. Lett. **52**, 1919 (1984)
11. D. Straub, F.J. Himpsel: Phys. Rev. Lett. **52**, 1922 (1984)
12. D. Straub, F.J. Himpsel: Phys. Rev. B **33**, 2256 (1986)
13. K. Giesen, F. Hage, F.J. Himpsel, H.J. Riess, W. Steinmann: Phys. Rev. Lett. **55**, 300 (1985)
14. K. Giesen, F. Hage, F.J. Himpsel, H.J. Riess, W. Steinmann: Phys. Rev. **35**, 971 (1987)
15. K. Giesen, F. Hage, F.J. Himpsel, H.J. Riess, W. Steinmann, N.V. Smith: Phys. Rev. B **35**, 975 (1987)
16. G.D. Kubiak: Surf. Sci. **201**, L 475 (1988)
17. S.D. Kevan: Phys. Rev. Lett. **50**, 526 (1983)
18. S. Schuppler, N. Fischer, E. Bertel, W. Steinmann: To be published
19. A. Goldmann, M. Donath, W. Altmann, V. Dose: Phys. Rev. B **32**, 837 (1985)
20. P.M. Echenique, F. Flores, F. Sols: Phys. Rev. Lett. **55**, 2348 (1985)
21. R.W. Schoenlein, J.G. Fujimoto, G.L. Eesley, T.W. Capehart: Phys. Rev. Lett. **61**, 2596 (1988)
22. H.B. Nielsen, G. Boström, E. Matthias: To be published
23. N.V. Smith: Phys. Rev. B **32**, 3549 (1985)
24. S.L. Hulbert, P.D. Johnson, N.G. Stoffel, W.A. Royer, N.V. Smith: Phys. Rev. B **31**, 6815 (1985)
25. S.L. Hulbert, P.D. Johnson, N.G. Stoffel, N.V. Smith: Phys. Rev. B **32**, 3451 (1985)
26. B. Reihl, K.H. Frank, R.R. Schlittler: Phys. Rev. B **30**, 7328 (1985)
27. A. Goldmann, V. Dose, G. Borstel: Phys. Rev. B **32**, 1971 (1985)
28. W. Altmann, V. Dose, A. Goldmann, U. Kolac, J. Rogozik: Phys. Rev. B **29**, 3015 (1984)
29. N. Garcia, B. Reihl, K.H. Frank, A.R. Williams: Phys. Rev. Lett. **54**, 591 (1985)
30. B. Reihl, J.M. Nicholls: Z. Phys. B **67**, 221 (1987)
31. D. Rieger, T. Wegehaupt, W. Steinmann: Phys. Rev. Lett. **58**, 1135 (1987)
32. T. Wegehaupt, D. Rieger, W. Steinmann: Phys. Rev. B **37**, 10086 (1988)